Kinetic and thermodynamic evaluation of effective combined promoters for CO_2 hydrate formation

Mohd Hafiz Abu Hassan[a,b], Farooq Sher[c,*], Gul Zarren[d], Norhidayah Suleiman[e], Asif Ali Tahir[f], Colin E. Snape[a]

a. *Department of Chemical and Environmental Engineering, University of Nottingham, University Park, Nottingham NG7 2RD, UK*

b. *Faculty of Science and Technology, Islamic Science University of Malaysia, Bandar Baru Nilai, 71800 Nilai, Negeri Sembilan, Malaysia*

c. *School of Mechanical, Aerospace and Automotive Engineering, Faculty of Engineering, Environmental and Computing, Coventry University, Coventry CV1 2JH, UK*

d. *Department of Chemistry, Government College Women University, Faisalabad 38000, Pakistan*

e. *Department of Food Technology, Faculty of Food Science and Technology, Universiti Putra Malaysia, 43400 UPM Serdang, Selangor, Malaysia*

f. *Environment and Sustainability Institute, University of Exeter, Penryn Campus, Cornwall TR10 9FE, UK*

Abstract

The increase in carbon dioxide (CO_2) concentration in the atmosphere raises earth's temperature. CO_2 emissions are closely related to human induced activities such as burning of fossil fuels and deforestation. So to make the environment sustainable, carbon capture and storage (CCS) is required to reduce CO_2 emissions. In this study, CO_2 hydrate (CO_2:$6H_2O$) formation has been explored as an approach to capture CO_2 in the integrated gasification combined cycle (IGCC) conditions. The formation of hydrate was experimentally investigated in an isochoric system with high-pressure volumetric analyzer (HPVA). The solubility of CO_2 in water using experimental

*Corresponding author:
E-mail address: Farooq.Sher@coventry.ac.uk (F.Sher); Tel.: +44 (0) 24 7765 7754

pressure–time (P-t) curves were analyzed to determine the formation of hydrate. Additionally, the effect of newly synthesized combined promoters and various driving forces were evaluated. The experimental results demonstrated that the CO_2 uptake expanded as ΔP expanded and designated combined promoters type T1-5 and type T3-2 were the two best, acquiring a uptake of 5.95 and 5.57 mmol of CO_2 per g of H_2O separately. Ethylene glycol mono-ethyl ether (EGME) was demonstrated to be a good option to THF when linked with SDS, with a CO_2 uptake of 5.45 mmol for the designated combined promoters T1A-2. Additionally, the total sum of CO_2 devoured through hydrate development maximize as the measure of water inside mesoporous silica increased. All results of the studied parameters confirmed the reliability of experiments and successful implementation.

Keywords: Global warming; Gas hydrate; CO_2 capture and storage (CCS); HPVA; combined promoters, thermodynamics and kinetics.

1 Introduction

The energy demands of the globe have increased very rapidly. Energy consumption rises day by day globally by increasing industries, electric automobiles and developing economic demands. According to recent scenario, the energy consumption demand will increase by one third over next 25 years and will become more than double in 2060 [1]. The increased demands of energy also caused a high level of greenhouse gas (GHG) emissions in the environment, therefore as a result increased global warming [2]. Due to increased global warming, the European Union (EU) set the reduction target of CO_2 emission at least by 80% until 2050 [3]. According to the International Plant Protection Convention (IPPC) fifth assessment report, the leading issue of global warming

has caused a rise in temperatures approximately by 1.50 °C due to human induced activities [4, 5]. Mainly, the sources of carbon dioxide (CO_2) emissions are industrial activities and thermal power plants [6]. Therefore, the issue to capture CO_2 emissions emitting from the industrial processes have gained increasing concern.

Different schemes were used in the past to reduce global warming specifically carbon emissions in which renewable energy technologies are very important [5, 7]. The process called carbon capture and storage (CCS) emerged as the most important technology to capture and store CO_2 emitting directly from power and chemical plants [8, 9]. This technology mainly involves separation, conditioning, transportation and storage of CO_2. This four-step technology first captures the contents with rich CO_2 from any industrial sources, then condense and liquefies CO_2 before transporting it to the storage site usually through a pipeline and geologically stored it in the formation site of deep saline [10]. Among the whole process, the separation step of CO_2 is the one with high energy taking pathway that accounts for about 75–80% of the total cost of CCS [11]. Still, CCS is being recognized as a vital technology with the least cost against climate change mitigation that will be able to limit global warming below 2 °C [12].

There are several new strategies developed in the past that can physically and chemically capture CO_2 using blended solution [13, 14], nanostructured membranes of polymers, zeolites and various carbon or inorganic nanocomposites [15], adsorption media, cryogenic systems [16], integrated gasification combined cycle (IGCC) [17], hydrate based gas separation (HBGS) [18] and chemical looping combustion [19]. In IGCC technology, synthetic gas is reformed from fossil fuels (coal, oil and nature gas). In spite of IGCC promising utilization, it faces a major challenge of high

separation cost of CO_2 from CO_2/H_2 product gas [20]. Hence, energy saving and inexpensive technologies are required to capture CO_2 efficiently. Among all of the above mentioned strategies hydrate based gas separation (HBGS) is one of the novels approaches to capture and store CO_2 with relatively low consumption of energy [21]. HBGS can be used for both pre and post-combustion from the fuel and flue gas respectively. Though, the process of HBGS is likely more appropriate for pre-combustion of CO_2 capture. This is because of the partial pressure of fuel gas (consisting of 40% of CO_2 and 60% H_2) is thousand times greater than that of flue gas (consisting of 17% of CO_2 and 83% N_2) in case of post-combustion capture [22].

Therefore, in this study HBGS has been chosen because of the continuous operation property of CO_2 hydrate formation which enables the treatment of large volumes of gaseous stream, less operating cost and recuperative ability of CO_2 capture about 99 mol% from the flue gas [23]. Recently Zheng et al. [24] stated that even at ambient temperature carbon dioxide molecules could be arrested and stored by using HBGS improved properties, it provides the leeway for industrialists to use this pathway for further industrial applications. The process of HBGS relies on the ability of gas hydrate formation that is formed by water molecules and CO_2, N_2, O_2, H_2 or natural gas component (methane or ethane) at low temperature (near about 237 K) and at elevated pressure of about 10–70 bar [25, 26]. CO_2 hydrate is formed in case of pure CO_2 gaseous system at a pressure range of 12.70–45 bar and temperature range of 273.20–283 K [27].

In the past, numerous parameters have been scrutinized to improve the efficiency of CO_2 uptake, less operational cost and ease of hydrate formation. The parameters used for the increased efficiency of CO_2 capture are mainly promoters, types of silica, experimental dynamic force,

98 height of the bed and amount of moisture content. These parameters were investigated by
99 employing a solid adsorbent approach in HBGS, which is most preferred method in the industry
100 for CCS [18, 28, 29]. Nambiar et al. [30] worked with the biodegradable porous materials that
101 enabled almost double rate of hydrates formation with only 50% water saturation level. While Park
102 et al. [31] used only porous silica gel which increased the gas uptake due to high availability of
103 surface area to increase water and gas contact. Li et al., [32] employed nano-sized Al_2O_3 and found
104 that gas separation efficiency was improved by approximately 43.62% due to micro-sized
105 particles.
106
107 In spite of the remarkable advancements in HBGS technology, however, this technology still
108 requires a large amount of energy for compression and extraction of CO_2 and decrease in optimum
109 conditions of temperature and pressure. Thus, different thermodynamic promoters were used in
110 the past to optimize the conditions of hydrate formation. These promoters include Cyclopentane
111 (CP) [33], Tetra-n-butyl ammonium Chloride (TBAC) [34], Tetra-n-butyl ammonium bromide
112 (TBAB) [35], Tetra-n-butyl ammonium fluoride (TBAF) [29] and Tetrahydrofuran (THF) [36].
113 However, despite the usage of these promoters, still the time taking for process of hydrate
114 formation and limited gaseous solubility in water restrict the successful application of CO_2 capture
115 schemes. That is why more investigation regarding the definite solution of this problem is required.
116 Therefore, the present study investigates two parameters i.e. best type of silica and novel combined
117 type promoters to evaluate their effect for hydrate formation. The main focus was to evaluate the
118 optimum hydrate based separation in the operating conditions of an integrated gasification
119 combined cycle. Herein, the fact is highlight that hydrate formation is possible in integrated
120 gasification combined cycle conditions. Furthermore, the hydrate formation driving force and non-

hydrate forming conditions especially in IGCC conditions were investigated with the employment of pure CO_2 gas.

2 Experimental

2.1 Materials

Tetrahydrofuran (THF), Ethylene glycol mono-ethyl ether (EGME), sodium dodecyl sulfate (SDS) and tetrabutylammonium bromide (TBAB) promoters with the purity of 99.70, 99.60, 99.90 and 97.50% respectively were purchased from Fisher Scientific. Silica gel with standard particle size of 200–500 μm, pore volume of 0.630 cm^3/g, surface area of 499 m^2/g and mean pore size of 5.14 nm were purchased from Fisher Scientific. Antifreeze was provided by ASDA. A member of Linde group i.e. BOC supplied Helium and Nitrogen gas for cleaning and controlling the valve of high pressure volumetric analyzer (HPVA).

2.2 Sample preparation

The adsorbent employed was standard because silica gel due its high porosity and reproducibility can supply a large amount of contact area between water and gas molecules in a short time. Thus, it increases the kinetics of hydrate formation and enhances the CO_2 uptake as compared to other adsorbents. Furthermore, it was noted that silica gel with chosen specific properties, as a solid adsorbent can effectively overcome the gas/water contact limitation where in the gas phase will have better contact with water dispersed in pores of silica gel [37]. Four methods were used for the preparation of wet silica gel, the method with the best result was reported in this study. For preparation, silica gel was initially dried inside the oven for one night at 200 ^oC, before the commencement of the experiment. Oven with the model of AX30 manufactured by Carbolite was used. Dry silica gel (0.50 g) was placed inside blender and water was added in excess (19 times

143 the mass of dry silica gel) so that the total mass of the mixture became 50 g. The silica gel and
144 water mixture were vigorously stirred at a speed of 37,000 rpm [38] by using a high-speed blender
145 for 90 seconds. Then, the mixture was left at atmospheric conditions until the final mass reached
146 equilibrium. To obtain the final moisture content, the final equilibrium mass was subtracted from
147 dry silica gel mass. Four promoter samples were named as; THF, EGME, TBAB and SDS. Each
148 promoter was diluted in water to obtain, SDS with 0.01 mol% concentration [39] and 3 mol%
149 concentration of THF [39].
150
151 The combined-promoter designated type named T1-5 (5.60 mol% THF + 0.01 mol% SDS), T3-2
152 (0.01 mol% SDS +0.10 mol% TBAB) and T1A-2 (0.10 mol% EGME +0.01 mol% SDS) were
153 used in analysis. The discovery of two new combined-promoters (designated types T3-2 and T1A-
154 2) in this work could provide more options for HBGS research field in future.
155 **Table *1*** summarizes the concentration required for each combined-promoter employed. 2.50 g of
156 silica gel was used to prepare each sample. Then promoter-water solution equal to 47.50 g was
157 added to make the total mass of dry silica gel-promoter-water mixture equal to 50 g. These samples
158 were prepared by implementing the highest rates of stirring. The degassing unit was used to
159 calculate an exact amount of moisture content residing inside the pores of silica gel. The amount
160 of water content was necessary to calculate the final conversion of water to CO_2 hydrate.

161 ## 2.3 Experimental procedure

162 Fig. 1 shows the work station for hydrate formation experiments consisting of a high-pressure
163 volumetric analyzer (model HPVA-100, manufactured by Micromeritics). It contains a computer
164 unit, a constant temperature bath, gas cylinders and a vacuum pump. The mixture of 70 vol% water
165 + 30 vol% antifreeze was used to avoid the formation of ice inside the temperature control vessel

and to make sure that the water mixture was consistently circulated throughout the process. Gas chambers were important to give an investigation of gas with 99.99% purity having 103 bar pressure and Helium gas with the same purity having 34.40 bar pressure for expelling and cleaning purposes. The pneumatic valves of HPVA were also controlled by the gas chambers. Prior to the initiation of analysis, to clean the line from any sort of polluting influences, physical cleaning of the system was done by gas.

The working conditions, such as; analyze time, examination gas port, working weight, and temperature were pre-characterized. From that point forward, the cells valve was firstly closed and sample cell was accused with silica gel having a sufficient amount of water that was placed inside the water bath. During the experimental work, the desired working temperature was built up through a steady temperature bath and simultaneously the required pressure was built up through a supply vessel. The cells valve was directed to completely open, after the maintenance of operating conditions. Then the analysis was done for 1200 minutes. At that point, the weight was diminished to barometrical pressure at the equivalent working temperature for hydrate disintegration. After that, the sample cell was removed from HPVA and the cells valve was allowed to completely shut. At long last, the development of hydrate in the HPVA was inspected by examining the P-t bends and furthermore the examination on CO_2 dissolution in water.

2.3.1 Uncertainty analysis

All prepared samples were used to investigate hydrate formation in the HPVA by using pure CO_2 gas (99.99% purity). The P-t curve for all experiments that exhibited hydrate formation either in pure CO_2 or fuel gas mixture showed a similar trend. In this study, the P-t (Pressure-time) curves obtained were determined through the formation of hydrate together with the study of CO_2

dissolution in water according to Henry's Law and then followed by the analysis of water conversion to hydrate, CO_2 uptake and rate of hydrate formation. All experiments were conducted for 1200 minutes to obtain maximum water conversion to hydrate and maximum CO_2 uptake. For accurate measurement, the rate of hydrate formation was reported every 30 minutes because the data was very large. The sampling time for data acquisition of pressure and temperature were taken every 5 s by HPVA. Thus, the rate for every 30 minutes helps for proper visualization of the rate change during 1200 minutes. Furthermore, to ensure the accuracy and statistical validity of the reported results two runs for each sample promoters were performed. However, the average differences, standard deviation and estimation of the uncertainty of mean maximum water conversion to hydrate and mean maximum CO_2 uptake data through the estimation of 90% confidence intervals (CI) calculated with the help online statistics calculator to verify the reported results.

3 Results and discussion

The prepared samples T1-5, T3-2, T1A-2 and standard silica gel with water (baseline experiment) was used to investigate hydrate formation in HPVA at 275–293 K and 22–36 bar by using pure CO_2 gas (99.99% purity). All experiments were conducted for 1200 minutes to obtain maximum CO_2 uptake. The P-t curve obtained was firstly used to justify the successful formation of hydrate together with the study of CO_2 dissolution in water and then followed by the analysis of CO_2 uptake and rate of hydrate formation. Due to the limitation of crystallizer in which the formation of hydrate could not be seen directly by the eyes, there was a necessity to justify the formation of hydrate. Subsequently, two methodologies were utilized to analyze the formation of hydrate; examination of P-t bends and investigation of CO_2 disintegration in the water suggested by Servio and Englezos, [40].

212

213 According to Tang et al. [41], there must be at least a two-stage pressure drop upon completion of
214 the experiment to ensure the formation of hydrate. The first stage of pressure drop indicates the
215 dissolution of CO_2 in water and the subsequent stages indicate hydrate growth. This trend was
216 observed for baseline experiment during the hydrate formation experiment at the constant
217 temperature of 275 K (Fig. 2), where the total pressure drop achieved after 1200 minutes was
218 around 2 bar. The complete dissolution of CO_2 in water inside silica gel pores was observed after
219 the pressure dropped approximately to 33.8 bar. As seen in Fig. 2, the first 120 minutes showed
220 two stages of pressure drop. Point **a-c** is considered the first stage of pressure drop. Initially, a
221 pressure drop from point **a-b** indicates that the dissolution of CO_2 in water happened around 5
222 minutes in which Sloan and Koh [42] stated that upon dissolution of gas in water, labile clusters
223 form immediately. Concurrently, labile clusters started to agglomerate by sharing faces, thus
224 increasing disorder which explained the little rise in pressure from point **b-c**. This process
225 continued until the size of the cluster agglomerate reached a critical value at point **c,** wherein Sloan
226 and Koh [42] said this was the point where primary nucleation happens. Also, Tang et al. [41]
227 described the time from point **a-c** as an induction time for hydrate formation. Moreover, the fast
228 induction time observed in this work was almost less than 10 minutes by employing FBR this
229 agrees with the one reported in the literature [18, 43, 44]. Then, the second stage of pressure drop
230 was observed immediately after point **c** and this significant pressure drop is known as the hydrate
231 growth stage. From point **c-d** sudden decrease in pressure was observed which is expected due to
232 the availability of enough driving force required for the growth of hydrate. Thus, the significant
233 two-stage pressure drop observed in the initial stage (the first 20 minutes) before being followed
234 by the second small pressure drop (until 100 minutes) until almost no more drop in pressure was

observed in batch FBR as indicated by point **e**, could be a basic guideline to determine the formation of CO_2 hydrate and CO_2 dissolution in water. After point **e**, several stages of pressure drop were observed for the sample before it became a plateau. For the sample prepared by the highest rates of stirring, the pressure became constant approximately after 700 minutes. Moreover, the growth of hydrate and the fast induction time around 5–10 minutes for hydrate formation validates by different studies conducted in the literature [18, 40, 41]. Since the formation of hydrate was justified, next to the study on final water to hydrate conversion, CO_2 uptake and rate of hydrate formation are presented in the next section.

3.1 Hydrate formation analysis

Hydrate formation experiments were investigated in the HPVA by using a prepared sample with approximately 0.50 g of wet silica. The hydration number of 5.75 [45] was used to calculate the water conversion to hydrate as 6 water molecules are needed to form CO_2 hydrate ($CO_2.6H_2O$). The sample prepared by the highest rates of stirring had the maximum water conversion to hydrate with a value of 40.50 ± 2.28 mol%. The amount of gas uptake was directly related to the amount of water conversion to hydrate. Hence, the gas uptake obtained for the prepared sample was the highest amount of CO_2 molecules with a value of 0.29 mmol. Additionally, it was observed that the sample with the greater equilibrium moisture contents yielded the maximum water conversion to hydrate.

Moreover, the sample prepared by the highest rates of stirring demonstrated the fastest kinetics in which the initial rate of hydrate formation was more than 0.05 mmol of CO_2/g of H_2O/min. Overall, the silica contacted with water from vigorous stirring showed the best results and reproducibility. Thus, the silica contacted with water was used as a baseline result for comparison purposes.

Additionally, in the hydrate forming region, the equilibrium mole fraction of CO_2 in water was reduced as temperature decreased [40]. Thus, highest solubility of CO_2 observed in the water at lowest temperature that was due to the existence of CO_2 hydrate. In contrast, the solubility of CO_2 in water reduced as the temperature increased in non-hydrate forming region. This trend was comparable to the equilibrium mole fraction of CO_2 in water as shown in the literature [46] which explains the non-existence of hydrate at elevated temperature.

3.2 Integrated gasification combined cycle (IGCC) process

Generally, most of the literature has investigated CO_2 hydrate formation from fuel gas mixture in non-IGCC operating conditions whereas experiments performed in this work used the IGCC conditions. Mostly, the operating conditions of the IGCC are in the range of 283–290 K and 20–70 bar (fuel gas mixture) and are outside the hydrate forming conditions. The minimum pressure required for CO_2 hydrate to form at 283 K is 30 bar (pure CO_2) as discovered by Servio and Englezos, [40]. Nevertheless, the initial investigation on the implementation of promoters directed our attention to the hydrate formation in non-hydrate forming conditions. Therefore, the focus of the study was to obtain optimum hydrate formation in the IGCC operating conditions. Hence, additional experimental parameters were investigated and reported which indicated that hydrate formation is possible in IGCC conditions. The experimental parameters that were studied include hydrate formation driving force (ΔP) and various non-hydrate forming conditions (temperature and pressure), especially in the IGCC conditions.

3.3 Effect of driving forces in hydrate forming region

A study was performed to investigate the effect of driving force (ΔP) on hydrate formation. Various operating pressures (36, 30 and 22 bar) in pure CO_2 gas were investigated at 275 K by employing silica contacted with different combined-promoters. T1-5 and T3-2 (0.01 mol% SDS + 0.10 mol%

TBAB) were preferably studied combined-promoters due to their great CO_2 uptake ability achieved at 275 K and 36 bar. Then, some additional experiments at 30 bar and 22 bar for T1-5 and T3-2 were performed. In each experiment, approximately 0.50 g wet silica was used and the investigations were performed in HPVA for 1200 minutes. Then, the results were compared with the baseline experiment at various driving forces.

The comparison of hydrate formation at various driving forces is illustrated in Fig. 3 and Fig. 4. Fig. 3 (a) and Fig. 3(b) shows that T3-2 had a highest water conversion to hydrate and CO_2 uptake at 275 K and 30 bar respectively followed by T1-5 and the baseline experiment. However, T1-5 demonstrated the best results at 275 K and 22 bar as shown in Fig. 4(a) and Fig. 4(b) with T3-2 and baseline experiment obtaining almost identical results. Table 2 summarizes the gas uptake obtained by each sample at various operating pressures. Generally, the gas uptake for all samples increased as the driving force (ΔP) increased from 5 to 19 bar with T1-5 demonstrating the best result at all driving force except at $\Delta P = 5$ bar. Combined-promoters designated type T1-5 gives the maximum value of CO_2 uptake up to 5.95 ± 0.21 mmol of CO_2 per g of H_2O as ΔP increased from 5 to 19 bar at constant temperature (275 K) that is in accord with the results reported in the literature [47]. Even though the gas uptake of T3-2 was the highest at this driving force which was almost 0.50 mmol of CO_2 per g of H_2O higher than T1-5. The total CO_2 molecules captured by T1-5 was the highest (0.17 mmol) which was 0.03 mmol higher than T3-2. This is expected due to the higher amount of available water molecules attained by T1-5, 1.30 mmol higher than T3-2. In past, Silva et al. [48] studied the formation of hydrate in pure CO_2 by using STR with SDS and THF as promoters. They inferred that if just SDS was utilized, clathrate hydrate was formed in a traditional manner yet when THF was combined with SDS in an ideal extent, it was possible to

observe crystals of THF hydrate which stabilized the framework and acted as a promoter of CO_2 hydrate. Moreover, Yang et al. [39] performed a study on phase equilibrium for the THF-CO_2-H_2O system which showed a drastic decrease in pressure in the presence of 3.00 mol% THF and SDS (at all concentrations). Also, the highest equilibrium temperature obtained was 291.55 K at 30 bar in the presence of 3.0 mol% THF and 0 mg/L SDS respectively. The experiments on hydrate formation have indicated that CO_2 hydrate forms rapidly at all experimental pressures when the SDS concentration is 1000 ppm which indicates that SDS enhances the hydrate formation rate.

In contrast to T1-5, the total CO_2 molecules captured by the baseline experiment were lower at all driving forces even though the amount of water molecules available for hydrate formation was higher than T1-5 by almost 0.50 mmol. However, the CO_2 molecules captured by the baseline experiment were higher than T3-2 at all driving forces except at $\Delta P = 13$ bar. In addition, at this medium driving force, T3-2 exhibited the closest result to T1-5. Hence, the results showed that high operating pressure enhanced the formation of hydrate due to greater driving force (ΔP). In addition, different samples had diverse effects on hydrate formation at different driving forces. In past, Kobayashi et al. [49] said a batch system is assumed to instantaneously keep itself in thermodynamic equilibrium and Mori et al. [50] referenced that the change in gas phase arrangement in batch mode is unavoidably convoyed by a change in the guest molecule composition in an instantaneously formed hydrate. These can be associated with a decrease in driving force in batch mode upon hydrate growth wherein in a pure CO_2 system, this effect was only observed when the initial operating pressure was below 30 bar. At high initial operating pressure (36 bar), a massive ratio of CO_2 to water molecules was expected to provide an extra driving force, which explained the high CO2 uptake, obtained.

3.3.1 Kinetic additives effect of hydrate formation

Generally, an increase in the driving force increases the gas uptake and kinetic rate of hydrate formation. Fig. 5 illustrates that the initial rate of clathrate formation of T3-2 at 275 K and 30 bar was the fastest that was 13% greater than T1-5 and almost 70% faster than the baseline experiment. However, the initial rate of clathrate formation at 275 K and 22 bar as shown in Fig. 6 was the fastest for T1-5 with the value of 0.012 mmol of CO_2 per g of H_2O per min followed by T3-2 (0.005 mmol of CO_2 per g of H_2O per min) and baseline experiment (0.004 mmol of CO_2 per g of H_2O per min). TBAB inhibit the hydrate formation but the combining promoter SDS used in the formation of T3-2 mitigate the inhibition effect of TBAB on hydrate formation only to some extent. Therefore, the rate of hydrate formation and CO_2 uptake of T3-2 is lower than that of T1-5. In view of these observations, it was inferred that THF displayed the quickest kinetics when it is joined with SDS of 0.01 mol%, practically more than half (50%) a solitary promoter alone at a similar concentration. In this way, it was affirmed that 0.01 mol% of SDS joined with THF gave the most maximum rate of clathrate formation and also CO_2 uptake due to reinforcing combined effect of promoters. Hence, T1-5 was proved to be the best option for hydrate formation at low driving force. These findings are in concurrence with the consequences of Kang et al. [51] who investigated the formation of hydrate in bulk water (cluster of water molecules) at different pressure and found that CO_2 uptakes increase as the operating pressure increased. In contrast, Zheng et al. [29] studied CO_2 semi clathrate formation under various concentration of promoters in HBGS at a driving temperature and reported that the CO_2 uptakes increase as the operating temperature sets up to 4.1 K. Thus, as ΔP increases or as ΔT decreases, the driving force also increases that indicates the successful formation of CO_2 hydrate.

3.4 Enhanced hydrate formation in non-hydrate forming region

The use of promoters could enhance hydrate formation as the baseline experiment did not show any hydrate formation at 288 K and 36 bar. Each promoter was extensively investigated by previous researchers where SDS [41] can avoid the development of obstructing hydrate film whilst TBAB [35] and THF [43] can form semi-clathrate and sII hydrates respectively. Both types of hydrate are said to entrap more CO_2 molecules in the small cage of sII hydrate and semi-clathrate hydrate cavities correspondingly [52]. Moreover, several researchers [53, 54] have investigated the effect of combining SDS and THF on CO_2 hydrate formation and they discovered that the synergic effect improves hydrate formation.

However, the synergic effect of combining SDS and TBAB has not yet been reported in the literature. Herein, the hydrate formation is investigated in non-hydrate forming region at 36 bar and various operating temperatures by employing pure CO_2 gas and novel combined-promoters. Yang et al. [39] plotted the phase equilibrium of hydrate formation in pure CO_2 gas system and showed that at 36 bar, the equilibrium temperature was 280 K. In this study, the operating temperature of 288 K led to the driving force of $\Delta T = 8$ K and for 293 K, $\Delta T = 13$ K. Unlike ΔP, the highest value of ΔT was equivalent to the lowest driving force available for the system because the operating conditions could be shifted to the right-hand side of phase equilibrium, also known as the non-hydrate forming region. This study was then used as a basis for the investigation of hydrate formation at IGCC plant operating conditions.

3.4.1 Combined promoters effect at various driving forces

Further investigation was performed by employing three combined-promoters (T1-5, T3-2 and T1A-2) at the 288 K and 36 bar operating conditions. Then, T1-5 and T3-2 were employed for the

investigation at 293 K and 36 bar. All experiments were conducted for 1200 minutes and 0.5 g of silica contacted with combined-promoter was used for each experiment. Fig. 7 (a) illustrates the conversion of water to hydrate at 288 K and 36 bar wherein T3-2 was found to show the best result with around 10 mol% conversion. This was followed by T1-5 and THF with both having a conversion around 9 mol%, followed by T1A-2 and SDS with around 6 mol% for both conversions. The water conversion to hydrate and gas uptake results for SDS and THF reported here are in accordance with the results reported in the literature [47]. Fig. 7 (b) and Table 3 show that the highest gas uptake was observed for T1-5 with the value of 1.25 mmol of CO_2 per g of H_2O followed by THF (1.15 mmol of CO_2 per g of H_2O), T3-2 (1.00 mmol of CO_2 per g of H_2O), T1A-2 (0.68 mmol of CO_2 per g of H_2O) and SDS (0.66 mmol of CO_2 per g of H_2O).

The results showed that by adding THF, TBAB and EGME to SDS, water conversion to the clathrate formation and the maximum gas uptake was increased accordingly. Significant improvement was observed when 5.60 mol% THF was added to 0.01 mol% SDS with almost double gas uptake obtained as compared to SDS (0.01 mol%) alone. In addition, during the study of hydrate phase equilibria of mixed hydrates having CO_2 and N_2, the gas uptake for 3 mol% THF alone was almost comparable to T1-5 which showed that THF was a very good promoter for hydrate formation at high temperature [55]. The same trend was observed for T3-2 in which 0.10 mol% TBAB was added to 0.01 mol% SDS. However, 0.1 mol% EGME only showed a minimal effect on hydrate formation when it was added to 0.01 mol% SDS. Based on the results obtained at these operating conditions, T1-5 and T3-2 were further investigated at 293 K and 36 bar. Fig. 8 (a) also demonstrates that T3-2 had the best water conversion to water entrapped clathrate with a conversion of around 6 mol% at temperature of 293 K and pressure of 36 bar. This was followed

by T1-5 being almost 50% lower than T3-2. Though, the maximum gas uptake for T1-5 was 0.03 CO_2 (mmol)/ H_2O (g) CO_2 per g of H_2O higher than T3-2 as presented in Fig. 8 (b) and Table 3. However, the maximum gas uptake for samples T1-5 and T3-2 reported in Fig. 8 (b) shows consistency within the estimated uncertainties of reported results.

The same trend was observed at both operating temperatures due to high equilibrium moisture content in T1-5 which was 50% higher than T3-2. Thus, T3-2 demonstrated the highest water conversion to hydrate as compared to T1-5 due to lower water presence inside silica gel pores. As a result, fewer CO_2 molecules were consumed in hydrate formation at 288 K for T3-2, which was 0.02 mmol less than T1-5. Moreover, slightly high error bars for T3-2 observed at these operating conditions, were due to regeneration experiment performed by reusing the same sample. However, other regeneration experiments demonstrated quite high regeneration values as shown in Table 3. Finally, the CO_2 molecules captured at 293 K were comparable for both samples which showed that THF and TBAB demonstrated the same effect at this operating temperature.

3.4.2 Kinetic additives effect of hydrate formation

Fig. 9 illustrates the rate of clathrate formation at 288 K and 36 bar where the addition of 5.60 mol% THF to form T1-5 significantly increased the initial kinetics of silica contacted with single SDS (0.01 mol%) from 0.005 to 0.015 mmol of CO_2 per g of H_2O per min. Moreover, the addition of 0.10 mol% TBAB and 0.10 mol% EGME in 0.01 mol% SDS also doubled the initial rate of hydrate formation for single SDS as illustrated by T3-2 and T1A-2 respectively. These indicated that the combination of other promoters with SDS enhanced the kinetics of hydrate formation known as a synergic effect. The synergic effect of T1-5 was obtained from SDS which avoided the development of obstructing hydrate film whilst THF formed sII hydrate which attracted more

418 CO_2 molecules for occupancy in small cages. The role of TBAB in T3-2 combined-promoter
419 provided more cavities for the occupancy of CO_2 molecules by forming semi-clathrate hydrate.
420 Moreover, the ability of TBAB to readily form semi-clathrate hydrate in hydrate forming
421 conditions caused TBA^+ to occupy large cage leaving the small cages empty/partially empty which
422 reduced the formation of CO_2 hydrate to 0.29 mol% of TBAB. Another EGME promoter was
423 considered as an alternative to THF due to the ability of EGME molecules to act as structure maker
424 solutes when dissolved in water. However, the gas uptake of EGME containing T1A-2 sample was
425 just 9% lower than T1-5 and the total CO_2 molecules consumed was only 0.05 mmol lower.
426 Therefore the initial kinetics of the sample that employed THF alone were faster than T3-2 and
427 T1A-2 and slightly slower than T1-5 which showed that THF was the best promoter to be
428 combined with SDS for enhancing clathrate formation. Even though the hydrate phase equilibrium
429 mitigated the hydrate forming region with the presence of combined-promoters, it significantly
430 affects CO_2 uptake and hydrate formation if temperature and pressure conditions changed below
431 or above to their respective optimum range. The hydrate phase equilibria promoting the lower
432 pressure and high temperature regions when the thermodynamic promoters were introduced. The
433 effect of promoters in mitigating hydrate phase equilibria to the hydrate forming region was
434 explained earlier in which THF and TBAB are known as thermodynamic promoters due to their
435 ability to form sII and semi-clathrate hydrates respectively that attracted more CO_2 molecules to
436 get involved in hydrate formation. Thus, this was the reason CO_2 uptake was almost 2 mmol of
437 CO_2 per g of H_2O when T1-5 and T3-2 combined-promoters were employed in FBR. Therefore,
438 at 293 K temperature and pressure condition of 36 bar, T1-5 and T3-2 demonstrated almost
439 comparable rates of hydrate formation as illustrated in Fig. 10. This indicated that at high
440 temperature, TBAB was the best alternative to THF to be employed together with SDS.

3.5 Thermodynamically shifted hydrate phase equilibrium in IGCC conditions

One of the most important findings in this work was the ability of combined-promoters to shift the hydrate phase equilibrium to a higher operating temperature. Fig. 11 demonstrates the hydrate phase equilibrium for pure CO_2. As the use of solid adsorbent for hydrate formation will lead to the use of a fluidized bed reactor (FBR). Previously, some works on the application of FBR by using pure CO_2 gas were performed by Yang et al. [39, 52], Mekala et al. [56] and Kumar et al. [37]. Kumar et al. [37] and Mekala et al. [56] investigated FBR (also known as HPVA) in which 0.25 mm silica gel and 0.46 mm silica sand (particle sizes) were employed respectively with no improvement in hydrate phase equilibrium compared to bulk water [57] as shown in Fig. 11.

However, Yang et al. [39, 52] managed to prove that the application of combined-promoters at optimum concentrations with 3 mol% of THF + 0.01 mol% SDS and equivalent concentration of THF + TBAB inside glass bead pores shifted the phase equilibrium to a higher temperature region (290 and 291 K respectively). In addition, Yang et al. [52] also discovered that both THF and TBAB showed the same role in thermodynamically shifting the phase equilibrium to a higher temperature region. At the same concentration of TBAB (5 mol%), the temperature increased from 286 to 291 K at operating pressure of 35 bar as the concentration of THF increased from 0–5 mol%. Also, at the same concentration of THF (5 mol%) and 35 bar, the temperature was observed to increase from 289 to 291 K as the concentration of TBAB increased from 0–5 mol%.

Moreover, Joshi et al. [58] reported that the addition of SDS did not mitigate the phase equilibrium of CO_2 -TBAB-H_2O system while Yang et al. [52] mentioned that SDS is known as a kinetic additive which can change the kinetic properties and has no influence on the hydrate phase

equilibrium [59]. Thus, the presence of thermodynamic promoters i.e. THF and TBAB in combined type promoters T1-5 and T3-2 respectively inside silica gel in this work (Table 1) promoted the phase equilibrium to 293 K and not the existence of 0.01 mol% SDS. Furthermore, the R square value of this study, interpreting from the fitness of data set, shows more goodness of fit with the value of 0.96 in comparison to the studies reported in the literature (Fig. 11).

4 Additives effect for CO_2 hydrate formation

In past, massive efforts have been done to enhance the driving forces and gas uptake of CO_2 hydrate formation by adding different thermodynamic and kinetic additives such as THF, SDS, tetra-butyl ammonium salts and Cyclopentane so that it can readily be applied for pre-combustion capture. THF and SDS can be effectively used to mitigate hydrate formation conditions, promote hydrate growth rate and improve separation efficiency. Ricaurte et al. [54] studied the effect of several additives on CO_2 hydrate formation in which SDS was paired with one of the thermodynamic promoters (THF, 1,3-dioxolane, 2-methyl-THF and CP) and THF was paired with one of the kinetic promoters (SDS, SDBS and DATCI). The results highlight that the combination of SDS and THF was the best for the formation of CO_2 hydrate from natural gas. However, Torre et al. [53] mentioned that the combination of THF and SDS compared to the single promoter was very advantageous in accelerating hydrate. Herslund et al. [60] presented new equilibrium data for the quaternary system H_2O-THF-CP-CO_2 which lowers equilibrium pressure of the system by 25-30% due to the formation of CP and THF hydrates simultaneously. Li et al. [61] discovered that the addition of CP into a TBAB solution remarkably enhanced the CO_2 separation and speed up the hydrate nucleation rate. While Yang et al. [52] performed a hydrate phase equilibrium investigation on various combinations of THF and TBAB concentrations in pure CO_2 gas system and found that the THF-TBAB system greatly shifted the hydrate phase equilibrium to the higher

488 temperature region around 291 K at an operating pressure of 42 bar. In spite of great advancement
489 in the study of additives, the investigations are limited to the application inside stirred tank reactor.
490 Therefore, some works must have been done to investigate the synergic effect of additives so that
491 the system can readily be applied in IGCC conditions and this study successfully finds a solution
492 and a way forward to utilize novel T1A-2 and T3-2 promoters in IGCC condition.
493

494 # 5 Conclusions

495 Three novel combined promoters namely T1-5, T3-2 and T1A-2 were investigated. The effect of
496 these combined promoters and various driving forces on the formation of CO_2 hydrates were
497 successfully investigated in IGCC conditions. Overall, the gas uptake for all samples in hydrate
498 forming conditions increased as the driving force (ΔP) of the pure CO_2 system increased.
499 Combined-promoters designated type T1-5 demonstrated the best result with the value of CO_2
500 uptake increasing from 0.86 ± 0.09 to 5.95 ± 0.21 mmol of CO_2 per g of H_2O as ΔP increased
501 from 5 to 19 bar at constant temperature (275 K). In contrast, the gas uptake was reduced from
502 5.95 ± 0.21 to 0.45 ± 0.07 mmol of CO_2 per g of H_2O as ΔT increased from -5 to 13 K at constant
503 pressure (36 bar). In general, the amount of available water inside silica gel pores determined total
504 number of CO_2 molecules captured through hydrate formation. Combined-promoters designated
505 type T3-2 captured the fewest CO_2 molecules at all driving forces due to the lowest amount of
506 available moisture content. However, T3-2 achieved an optimum result at CO_2 partial pressure of
507 30 bar (identical to the IGCC operating pressure of 70 bar) where the total number of CO_2
508 molecules captured were 0.01 mmol higher than the baseline experiment (0.13 mmol) due to
509 synergic effect. Thus, the study on non-hydrate forming region by employing pure CO_2 gas led to
510 the selection of 283 K and 36 bar as the operating conditions in IGCC by employing pure CO_2

511 wherein combined-promoters designated types T3-2 were chosen as an adsorbent to enhance CO_2
512 capture by HBGS technique. Conclusively these results recommend that several improvements
513 can be considered to improve hydrate formation in the IGCC conditions by considering different
514 factors that were discussed in this work. In future, the study on the selectivity of CO_2 gas molecules
515 towards hydrate formation in fuel gas mixture by gas chromatography (GC) analysis and the
516 improvement of reactor configuration by employing macroporous or mesoporous silicas (silica
517 sand or gel) with combined-promoters are suggested.
518

References

[1] H.-W. Schiffer, T. Kober, E. Panos, World Energy Council's Global Energy Scenarios to 2060, Zeitschrift für Energiewirtschaft, 42 (2018) 91-102.

[2] S.P. Mathur, A. Arya, Impact of Emission Trading on Optimal Bidding of Price Takers in a Competitive Energy Market, in: Harmony Search and Nature Inspired Optimization Algorithms, Springer, 2019, pp. 171-180.

[3] A. Antenucci, G. Sansavini, Extensive CO2 recycling in power systems via Power-to-Gas and network storage, Renewable and Sustainable Energy Reviews, 100 (2019) 33-43.

[4] C.J. Rhodes, Only 12 years left to readjust for the 1.5-degree climate change option–Says International Panel on Climate Change report: Current commentary, Science Progress, 102 (2019) 73-87.

[5] F. Sher, S.Z. Iqbal, H. Liu, M. Imran, C.E. Snape, Thermal and kinetic analysis of diverse biomass fuels under different reaction environment: A way forward to renewable energy sources, Energy Conversion and Management, 203 (2020) 112266.

[6] M.D. Aminu, S.A. Nabavi, C.A. Rochelle, V. Manovic, A review of developments in carbon dioxide storage, Applied Energy, 208 (2017) 1389-1419.

[7] S.P. Mathur, A. Arya, M. Dubey, A review on bidding strategies and market power in a competitive energy market, in: 2017 International Conference on Energy, Communication, Data Analytics and Soft Computing (ICECDS), IEEE, 2017, pp. 1370-1375.

[8] R. Bellamy, J. Lezaun, J. Palmer, Perceptions of bioenergy with carbon capture and storage in different policy scenarios, Nature communications, 10 (2019) 743.

[9] I.U. Hai, F. Sher, G. Zarren, H.J.J.o.C.P. Liu, Experimental investigation of tar arresting techniques and their evaluation for product syngas cleaning from bubbling fluidized bed gasifier, 240 (2019) 118239.

[10] Y. Tan, W. Nookuea, H. Li, E. Thorin, J. Yan, Property impacts on Carbon Capture and Storage (CCS) processes: A review, Energy Conversion and Management, 118 (2016) 204-222.

[11] A.A. Olajire, CO2 capture and separation technologies for end-of-pipe applications–a review, Energy, 35 (2010) 2610-2628.

[12] M. Bui, C.S. Adjiman, A. Bardow, E.J. Anthony, A. Boston, S. Brown, P.S. Fennell, S. Fuss, A. Galindo, L.A. Hackett, Carbon capture and storage (CCS): the way forward, Energy & Environmental Science, 11 (2018) 1062-1176.

[13] H. Li, Z. Zhang, Mining the intrinsic trends of CO2 solubility in blended solutions, Journal of CO2 Utilization, 26 (2018) 496-502.

[14] I.U. Hai, F. Sher, A. Yaqoob, H.J.F. Liu, Assessment of biomass energy potential for SRC willow woodchips in a pilot scale bubbling fluidized bed gasifier, 258 (2019) 116143.

[15] Y. Han, Z. Zhang, Nanostructured Membrane Materials for CO2 Capture: A Critical Review, Journal of nanoscience and nanotechnology, 19 (2019) 3173-3179.

[16] J. Xu, W. Lin, A CO2 cryogenic capture system for flue gas of an LNG-fired power plant, International Journal of Hydrogen Energy, 42 (2017) 18674-18680.

[17] A.-M. Cormos, C. Dinca, C.-C. Cormos, Multi-fuel multi-product operation of IGCC power plants with carbon capture and storage (CCS), Applied Thermal Engineering, 74 (2015) 20-27.

[18] J. Zheng, Y.K. Lee, P. Babu, P. Zhang, P. Linga, Impact of fixed bed reactor orientation, liquid saturation, bed volume and temperature on the clathrate hydrate process for pre-combustion carbon capture, Journal of Natural Gas Science and Engineering, 35 (2016) 1499-1510.

563 [19] L. Zhu, Y. He, L. Li, P. Wu, Tech-economic assessment of second-generation CCS: Chemical
564 looping combustion, Energy, 144 (2018) 915-927.
565 [20] X.-S. Li, Z.-M. Xia, Z.-Y. Chen, K.-F. Yan, G. Li, H.-J. Wu, Gas hydrate formation process
566 for capture of carbon dioxide from fuel gas mixture, Industrial & Engineering Chemistry Research,
567 49 (2010) 11614-11619.
568 [21] L. Li, S. Fan, Q. Chen, G. Yang, J. Zhao, N. Wei, Y. Wen, Experimental and modeling phase
569 equilibria of gas hydrate systems for post-combustion CO2 capture, Journal of the Taiwan Institute
570 of Chemical Engineers, 96 (2019) 35-44.
571 [22] R. Davidson, Pre-combustion capture of CO2 in IGCC plants, IEA Clean Coal Centre, (2011)
572 98.
573 [23] P. Babu, R. Kumar, P. Linga, Pre-combustion capture of carbon dioxide in a fixed bed reactor
574 using the clathrate hydrate process, Energy, 50 (2013) 364-373.
575 [24] J. Zheng, P. Zhang, P. Linga, Semiclathrate hydrate process for pre-combustion capture of
576 CO2 at near ambient temperatures, Applied energy, 194 (2017) 267-278.
577 [25] A. Li, J. Wang, B. Bao, High-efficiency CO2 capture and separation based on hydrate
578 technology: A review, Greenhouse Gases: Science and Technology, 9 (2019) 175-193.
579 [26] D.M. D'Alessandro, B. Smit, J.R. Long, Carbon dioxide capture: prospects for new materials,
580 Angewandte Chemie International Edition, 49 (2010) 6058-6082.
581 [27] J. Carrol, Natural Gas Hydrates, a Guide for Engineer. Gulf Prof. Publ, in, Elsevier,
582 Amsterdam, 2003.
583 [28] J. Yan, Y.-Y. Lu, J.-L. Wang, S.-L. Qing, Y.-R. Wang, Experimental investigation of
584 precombustion CO2 capture using a fixed bed of coal particles in the presence of tetrahydrofuran,
585 Energy & Fuels, 30 (2016) 6570-6577.
586 [29] J. Zheng, K. Bhatnagar, M. Khurana, P. Zhang, B.-Y. Zhang, P. Linga, Semiclathrate based
587 CO2 capture from fuel gas mixture at ambient temperature: Effect of concentrations of tetra-n-
588 butylammonium fluoride (TBAF) and kinetic additives, Applied Energy, 217 (2018) 377-389.
589 [30] A. Nambiar, P. Babu, P. Linga, CO2 capture using the clathrate hydrate process employing
590 cellulose foam as a porous media, Canadian Journal of Chemistry, 93 (2015) 808-814.
591 [31] S. Park, S. Lee, Y. Lee, Y. Lee, Y. Seo, Hydrate-based pre-combustion capture of carbon
592 dioxide in the presence of a thermodynamic promoter and porous silica gels, International Journal
593 of Greenhouse Gas Control, 14 (2013) 193-199.
594 [32] Z.-Y. Li, Z.-M. Xia, X.-S. Li, Z.-Y. Chen, J. Cai, G. Li, T. Lv, Hydrate-Based CO2 Capture
595 from Integrated Gasification Combined Cycle Syngas with Tetra-n-butylammonium Bromide and
596 Nano-Al2O3, Energy & fuels, 32 (2018) 2064-2072.
597 [33] L. Shifeng, F. Shuanshi, W. Jinqu, L. Xuemei, W. Yanhong, Clathrate hydrate capture of CO2
598 from simulated flue gas with cyclopentane/water emulsion, Chinese Journal of Chemical
599 Engineering, 18 (2010) 202-206.
600 [34] D.-L. Zhong, W.-C. Wang, Y.-Y. Lu, J. Yan, Using Tetra-n-butyl Ammonium Chloride
601 Semiclathrate Hydrate for Methane Separation from Low-concentration Coal Mine Gas, Energy
602 Procedia, 105 (2017) 4854-4858.
603 [35] P. Babu, W.I. Chin, R. Kumar, P. Linga, Systematic evaluation of tetra-n-butyl ammonium
604 bromide (TBAB) for carbon dioxide capture employing the clathrate process, Industrial &
605 Engineering Chemistry Research, 53 (2014) 4878-4887.
606 [36] A. Kumar, H.P. Veluswamy, R. Kumar, P. Linga, Kinetic promotion of mixed methane-THF
607 hydrate by additives: Opportune to energy storage, Energy Procedia, 158 (2019) 5287-5292.

[37] A. Kumar, T. Sakpal, P. Linga, R. Kumar, Influence of contact medium and surfactants on carbon dioxide clathrate hydrate kinetics, Fuel, 105 (2013) 664-671.
[38] R. Dawson, L.A. Stevens, O.S. Williams, W. Wang, B.O. Carter, S. Sutton, T.C. Drage, F. Blanc, D.J. Adams, A.I. Cooper, 'Dry bases': carbon dioxide capture using alkaline dry water, Energy & Environmental Science, 7 (2014) 1786-1791.
[39] M. Yang, Y. Song, W. Liu, J. Zhao, X. Ruan, L. Jiang, Q. Li, Effects of additive mixtures (THF/SDS) on carbon dioxide hydrate formation and dissociation in porous media, Chemical Engineering Science, 90 (2013) 69-76.
[40] P. Servio, P. Englezos, Effect of temperature and pressure on the solubility of carbon dioxide in water in the presence of gas hydrate, Fluid phase equilibria, 190 (2001) 127-134.
[41] J. Tang, D. Zeng, C. Wang, Y. Chen, L. He, N. Cai, Study on the influence of SDS and THF on hydrate-based gas separation performance, Chemical Engineering Research and Design, 91 (2013) 1777-1782.
[42] E.D. Sloan, C.A. Koh, Clathrate hydrates of natural gases third edition, CHEMICAL INDUSTRIES-NEW YORK THEN BOCA RATON-MARCEL DEKKER THEN CRC PRESS-, 119 (2008).
[43] P. Babu, C.Y. Ho, R. Kumar, P. Linga, Enhanced kinetics for the clathrate process in a fixed bed reactor in the presence of liquid promoters for pre-combustion carbon dioxide capture, Energy, 70 (2014) 664-673.
[44] P. Linga, R. Kumar, P. Englezos, Gas hydrate formation from hydrogen/carbon dioxide and nitrogen/carbon dioxide gas mixtures, Chemical engineering science, 62 (2007) 4268-4276.
[45] P. Babu, P. Linga, R. Kumar, P. Englezos, A review of the hydrate based gas separation (HBGS) process for carbon dioxide pre-combustion capture, Energy, 85 (2015) 261-279.
[46] L.W. Diamond, N.N. Akinfiev, Solubility of CO2 in water from− 1.5 to 100 C and from 0.1 to 100 MPa: evaluation of literature data and thermodynamic modelling, Fluid phase equilibria, 208 (2003) 265-290.
[47] M.H.A. Hassan, C.E. Snape, L. Steven, The effect of silica particle sizes and promoters to equilibrium moisture content for CO2 hydrate formation in HPVA, in: AIP Conference Proceedings, AIP Publishing, 2018, pp. 030019.
[48] C.F. da Silva Lirio, F.L.P. Pessoa, A.M.C. Uller, Storage capacity of carbon dioxide hydrates in the presence of sodium dodecyl sulfate (SDS) and tetrahydrofuran (THF), Chemical Engineering Science, 96 (2013) 118-123.
[49] T. Kobayashi, Y.H. Mori, Thermodynamic simulations of hydrate formation from gas mixtures in batch operations, Energy conversion and management, 48 (2007) 242-250.
[50] Y.H. Mori, N. Komae, A note on the evaluation of the guest-gas uptake into a clathrate hydrate being formed in a semibatch-or batch-type reactor, Energy Conversion and Management, 49 (2008) 1056-1062.
[51] S.-P. Kang, J. Lee, Y. Seo, Pre-combustion capture of CO2 by gas hydrate formation in silica gel pore structure, Chemical engineering journal, 218 (2013) 126-132.
[52] M. Yang, W. Jing, P. Wang, L. Jiang, Y. Song, Effects of an additive mixture (THF+ TBAB) on CO2 hydrate phase equilibrium, Fluid Phase Equilibria, 401 (2015) 27-33.
[53] J.-P. Torré, D. Haillot, S. Rigal, R. de Souza Lima, C. Dicharry, J.-P. Bedecarrats, 1, 3 Dioxolane versus tetrahydrofuran as promoters for CO2-hydrate formation: Thermodynamics properties, and kinetics in presence of sodium dodecyl sulfate, Chemical Engineering Science, 126 (2015) 688-697.

[54] M. Ricaurte, C. Dicharry, X. Renaud, J.-P. Torré, Combination of surfactants and organic compounds for boosting CO2 separation from natural gas by clathrate hydrate formation, Fuel, 122 (2014) 206-217.
[55] S.-P. Kang, H. Lee, C.-S. Lee, W.-M. Sung, Hydrate phase equilibria of the guest mixtures containing CO2, N2 and tetrahydrofuran, Fluid Phase Equilibria, 185 (2001) 101-109.
[56] P. Mekala, M. Busch, D. Mech, R.S. Patel, J.S. Sangwai, Effect of silica sand size on the formation kinetics of CO2 hydrate in porous media in the presence of pure water and seawater relevant for CO2 sequestration, Journal of Petroleum Science and Engineering, 122 (2014) 1-9.
[57] J. Carroll, Natural gas hydrates (a guide for engineers), Second Edition ed., Elsevier Inc USA: Burlington, 2009.
[58] A. Joshi, J.S. Sangwai, K. Das, N.A. Sami, Experimental investigations on the phase equilibrium of semiclathrate hydrates of carbon dioxide in TBAB with small amount of surfactant, International Journal of Energy and Environmental Engineering, 4 (2013) 11.
[59] A. Kumar, G. Bhattacharjee, B. Kulkarni, R. Kumar, Role of surfactants in promoting gas hydrate formation, Industrial & Engineering Chemistry Research, 54 (2015) 12217-12232.
[60] P.J. Herslund, K. Thomsen, J. Abildskov, N. Von Solms, A. Galfré, P. Brântuas, M. Kwaterski, J.-M. Herri, Thermodynamic promotion of carbon dioxide–clathrate hydrate formation by tetrahydrofuran, cyclopentane and their mixtures, International Journal of Greenhouse Gas Control, 17 (2013) 397-410.
[61] X.-S. Li, C.-G. Xu, Z.-Y. Chen, J. Cai, Synergic effect of cyclopentane and tetra-n-butyl ammonium bromide on hydrate-based carbon dioxide separation from fuel gas mixture by measurements of gas uptake and X-ray diffraction patterns, international journal of hydrogen energy, 37 (2012) 720-727.

List of Tables

Table 1. The amount of promoters used to prepare each combined-promoter (brief description of each code T1-5, T3-2 and T1A-2).

No.	Type of combined-promoter	Concentration and mass of promoter								Mass of water (g)
		THF		SDS		TBAB		EGME		
		mol%	g	mol%	g	mol%	g	mol%	g	
1	T1-5	5.60	9.11	0.01	0.07	-	-	-	-	38.39
2	T3-2	-	-	0.01	0.08	0.10	0.84	-	-	46.66
3	T1A-2	-	-	0.01	0.08	-	-	0.10	0.23	47.26

Table 2. Comparison of gas uptake for T1-5, T3-2 and baseline experiment at 275 K and 36, 30 and 22 bar in 1200 minutes.

Operating conditions	Sample	Exp. No.	No. of moles of water (mmol)	CO_2 formed in hydrate (mmol)	Mean CO_2 formed in hydrate (mmol)	CO_2 uptake (mmol of CO_2/g of H_2O)	Mean CO_2 uptake (mmol of CO_2/g of H_2O) (90% CI)	SD
275 K and 36 bar	T1-5	1	3.70	0.39	0.40	5.82	5.95 ± 0.21	0.18
		2	3.70	0.41		6.08		
	T3-2	1	2.40	0.23	0.24	5.36	5.57 ± 0.34	0.29
		2	2.40	0.25		5.77		
	SiG-H_2O	1	4.10	0.29	0.31	3.93	4.04 ± 0.17	0.15
		2	4.30	0.32		4.14		
275 K and 30 bar	T1-5	1	3.70	0.15	0.17	2.62	2.81 ± 0.30	0.26
		2	3.70	0.18		2.99		
	T3-2	1	2.40	0.13	0.14	3.09	3.28 ± 0.31	0.27
		2	2.40	0.15		3.47		
	SiG-H_2O	1	4.20	0.14	0.13	1.82	1.71 ± 0.19	0.16
		2	4.10	0.12		1.60		
275 K and 22 bar	T1-5	1	3.70	0.05	0.05	0.91	0.86 ± 0.09	0.08
		2	3.70	0.04		0.80		
	T3-2	1	2.40	0.01	0.01	0.35	0.30 ± 0.09	0.08
		2	2.40	0.01		0.24		
	SiG-H_2O	1	4.10	0.02	0.03	0.28	0.32 ± 0.06	0.05
		2	4.20	0.03		0.35		

Table 3. The comparison of gas uptake at 36 bar and operating temperatures of 288 K and 293 K in 1200 minutes.

Operating conditions	Sample	Exp. No.	No. of moles of water (mmol)	CO_2 formed in hydrate (mmol)	Mean CO_2 formed in hydrate (mmol)	Water conversion to hydrate (mol%)	Mean water conversion to hydrate (mol%)	CO_2 uptake (mmol of CO_2/g of H_2O)	Mean CO_2 uptake (mmol of CO_2/g of H_2O) (90% CI)	SD
288 K and	T1-5	1	3.70	0.07	0.07			1.26	1.25 ± 0.01	0.01
36 bar		2 [r]	3.70	0.07				1.24		
	T3-2	1	2.40	0.05	0.05			1.12	1.00 ± 0.20	0.17
		2[r]	2.40	0.04				0.88		
	T1A-2	1	3.50	0.05	0.05			0.76	0.68 ± 0.13	0.11
		2 [r]	3.50	0.04				0.60		
	SiG-	1	3.50	0.06	0.07			1.17	1.15 ± 0.03	0.03
	THF	2	3.50	0.07				1.13		
	SiG-	1	3.70	0.04	0.04			0.62	0.66 ± 0.06	0.05
	SDS	2	3.60	0.04				0.69		
293 K and	T1-5	1	3.70	0.02	0.02			0.41	0.45 ± 0.07	0.06
36 bar		2 [r]	3.70	0.02				0.49		
	T3-2	1	2.40	0.02	0.03			0.41	0.42 ± 0.01	0.01
		2	2.30	0.03				0.42		

[r] regeneration experiment

List of Figures

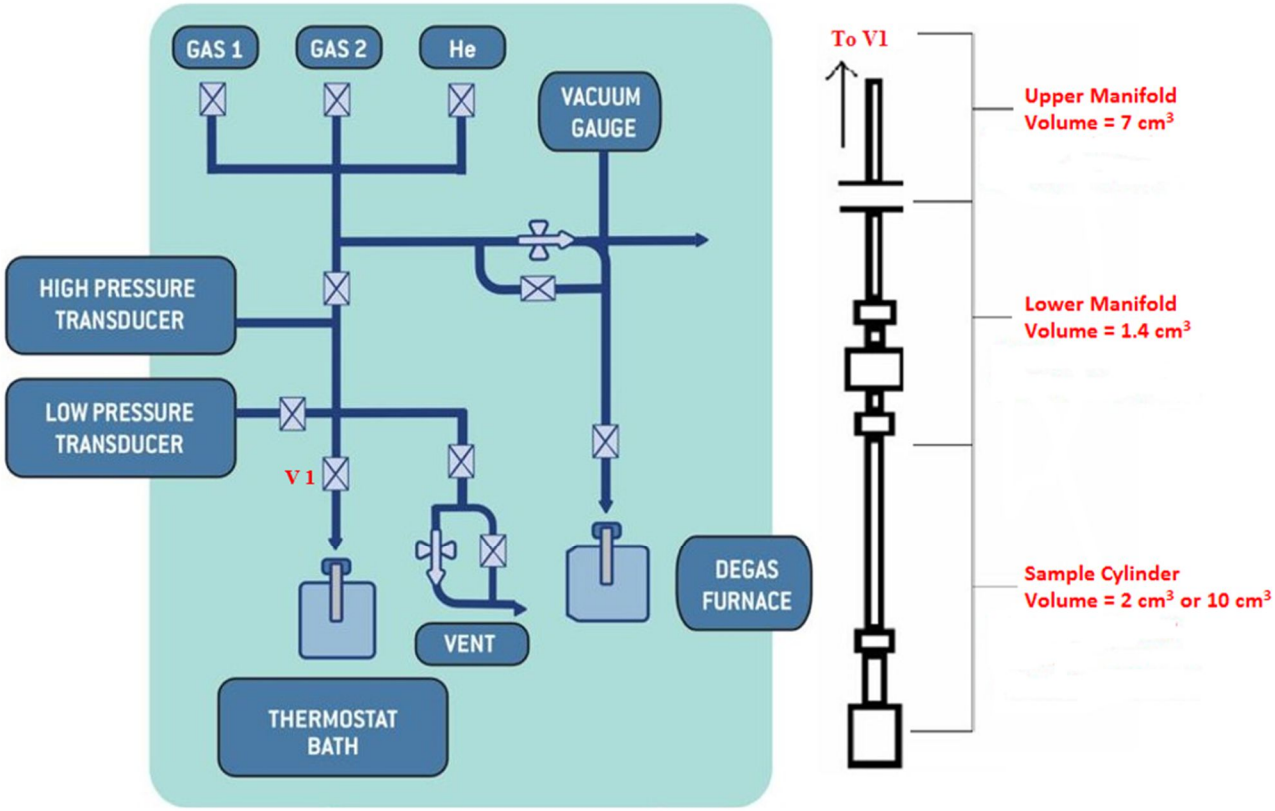

Fig. 1. Schematic representation of HPVA for hydrate formation.

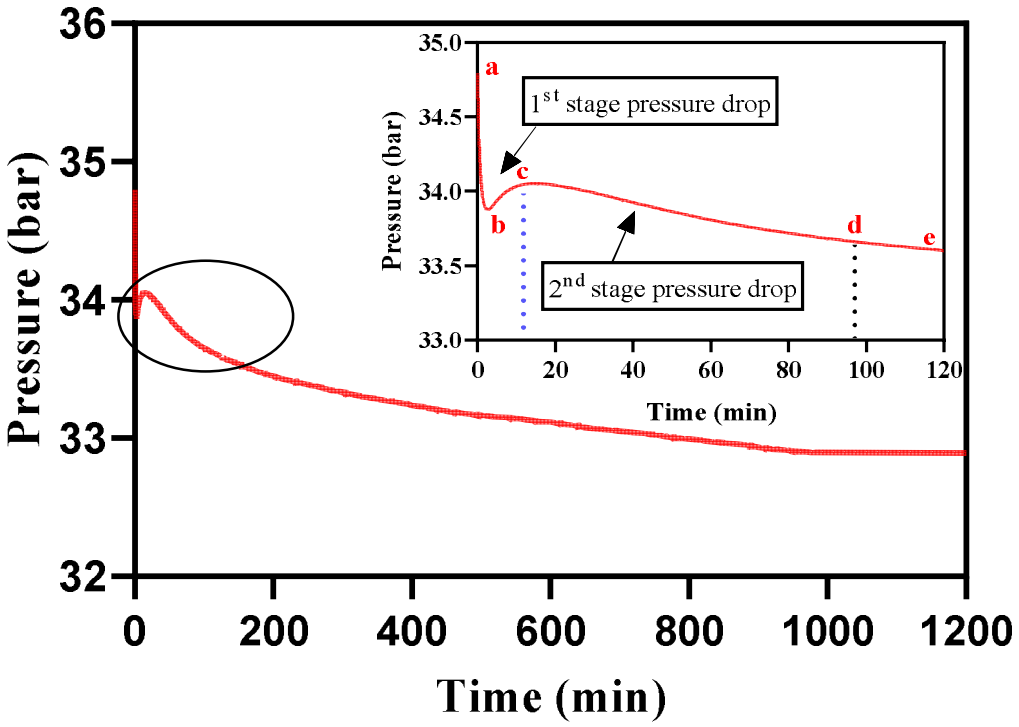

Fig. 2. P-t curves show 2-stage pressure drop in 1200 min for standard silica gel sample.

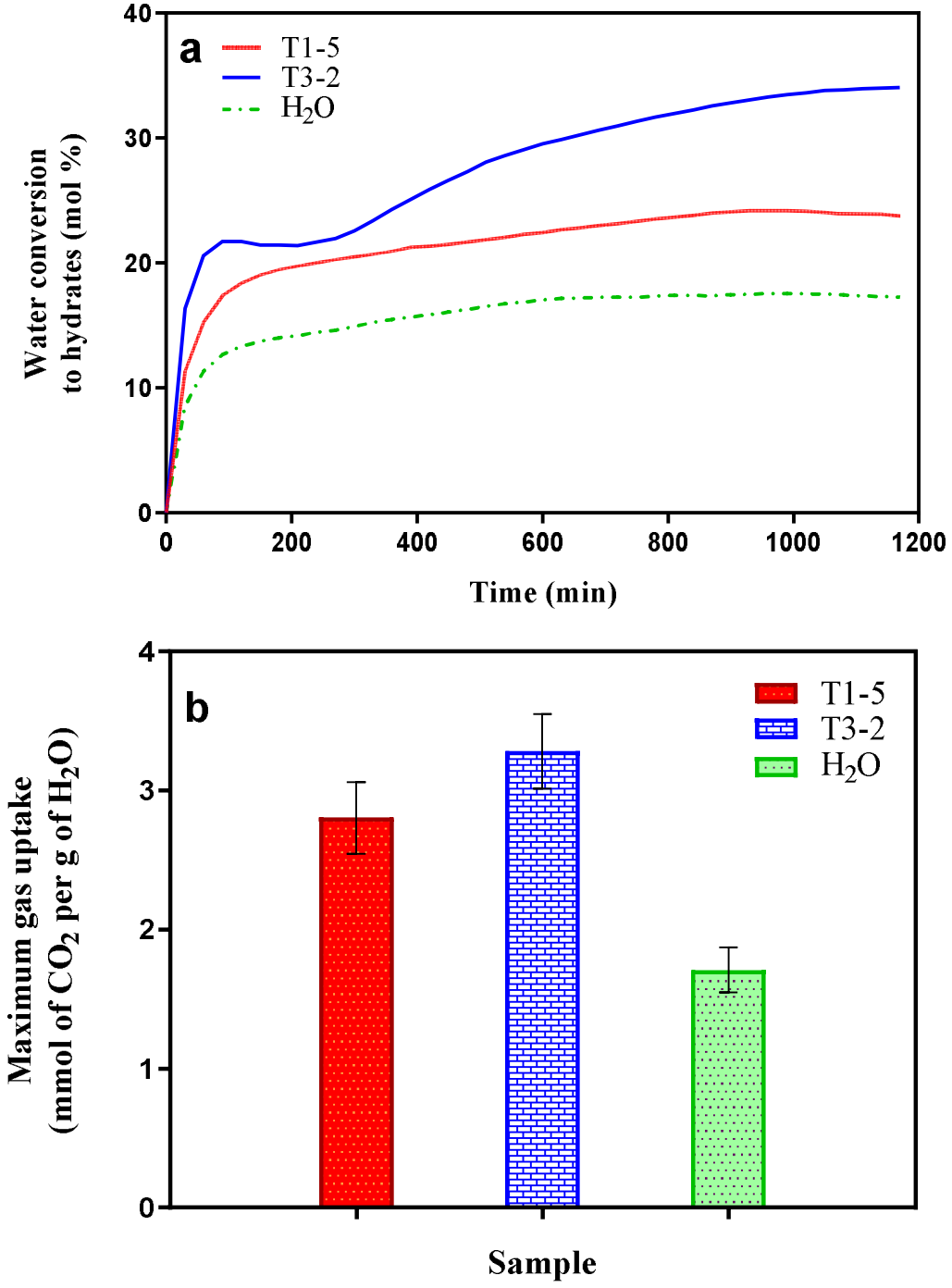

Fig. 3. Comparison of experiments at 275 K and 30 bar in 1200 min; (a) Water conversion to hydrate, (b) Gas uptake for T1-5, T3-2 and baseline.

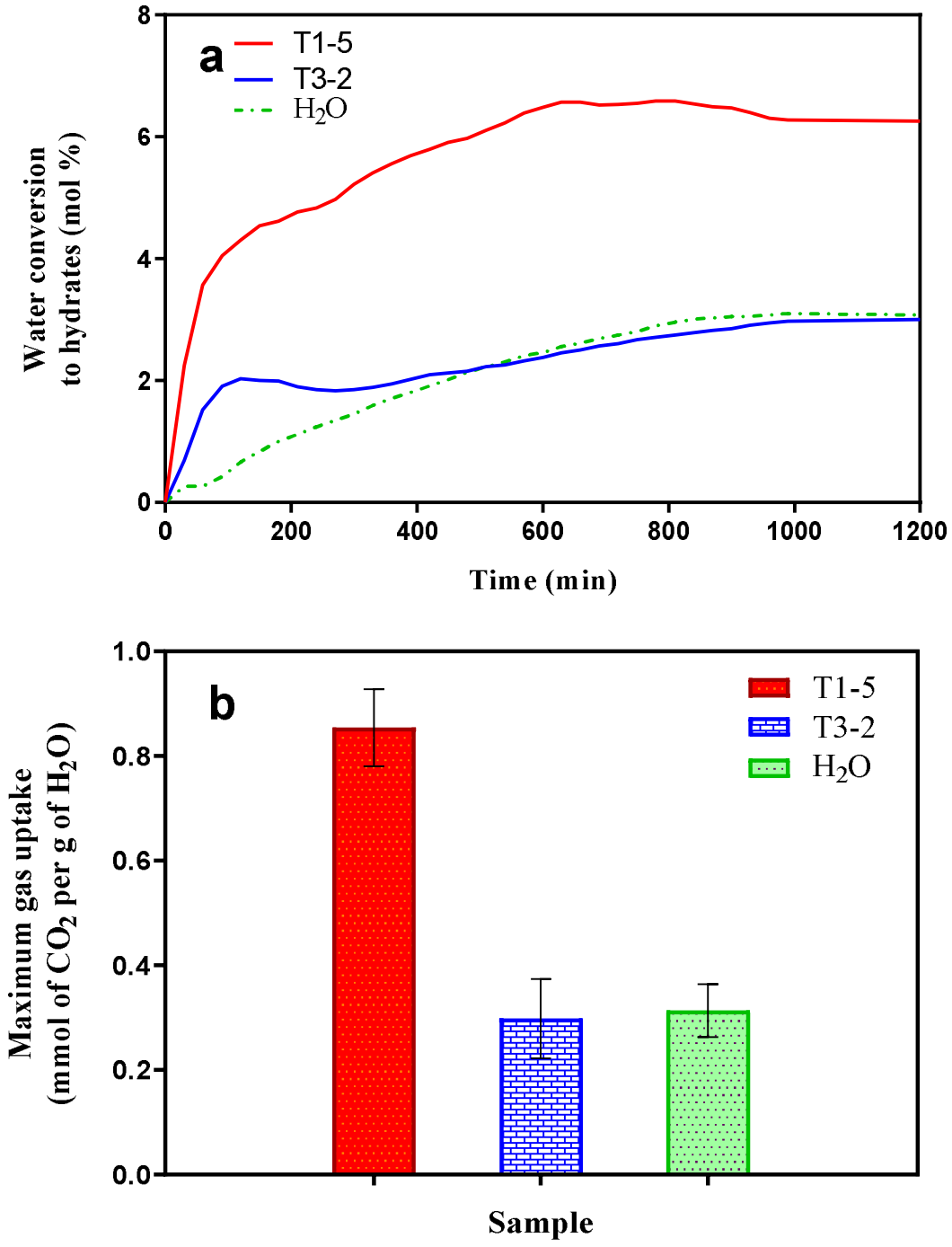

Fig. 4. Comparison of experiments at 275 K and 22 bar in 1200 min; (a) Water conversion to hydrate, (b) Gas uptake for T1-5, T3-2 and baseline.

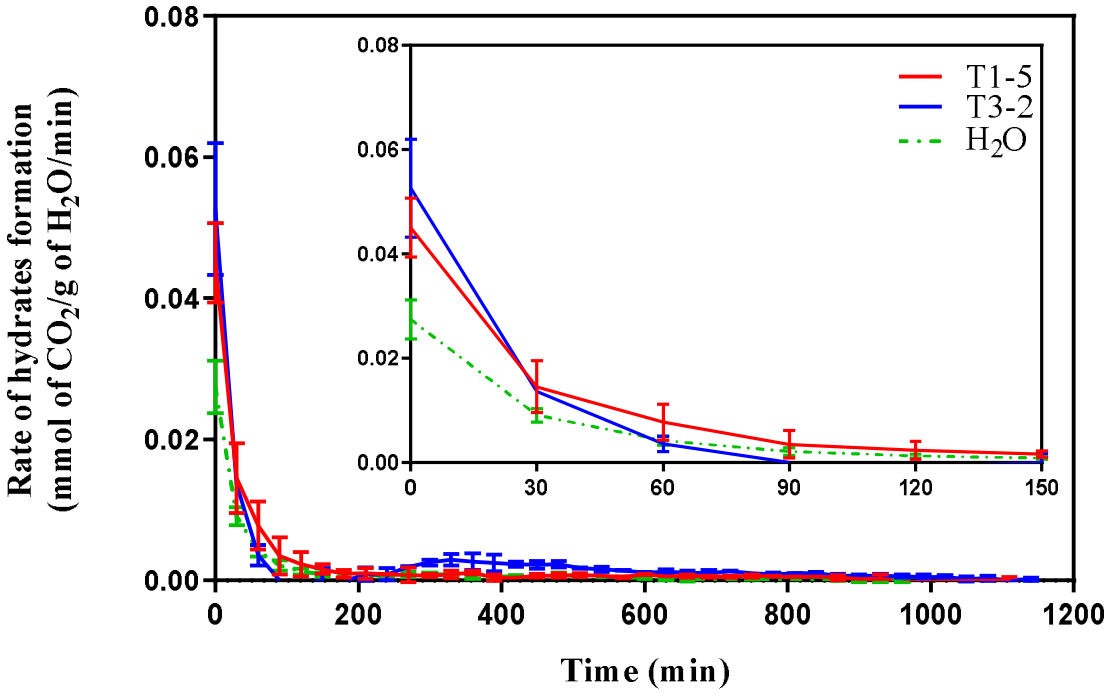

Fig. 5. Rate of hydrate formation at 275 K and 30 bar for 1200 minutes and inset for the first 150 minutes (T1-5, T3-2 and baseline experiment).

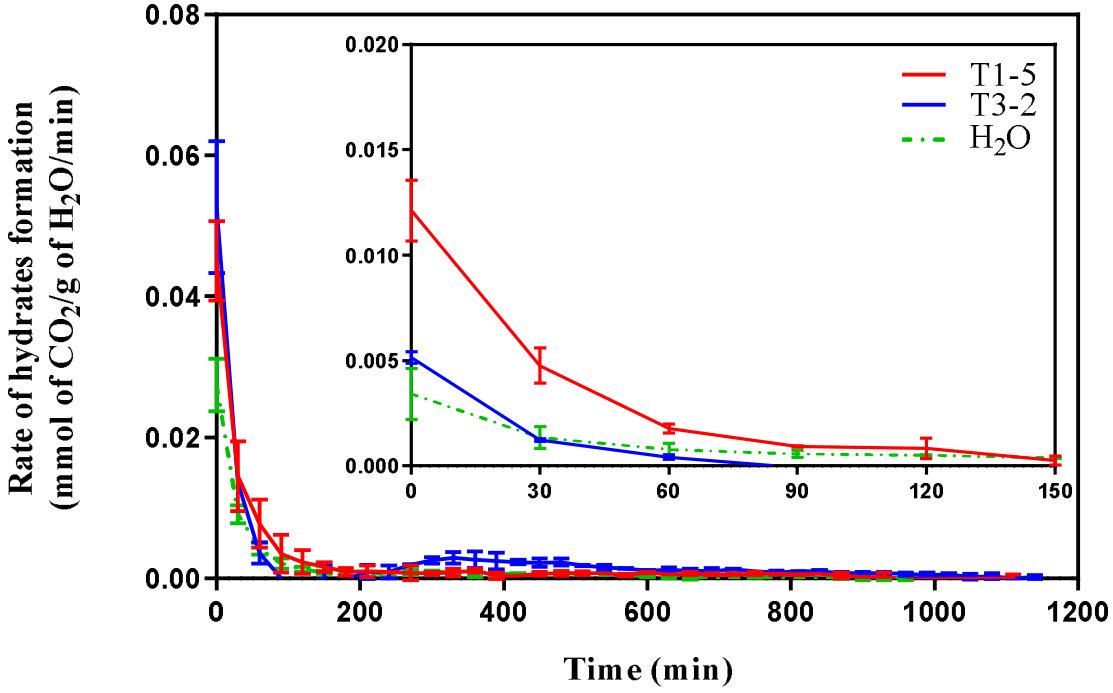

Fig. 6. Rate of hydrate formation at 275 K and 22 bar for 1200 minutes and inset for the first 150 minutes (T1-5, T3-2 and baseline experiment).

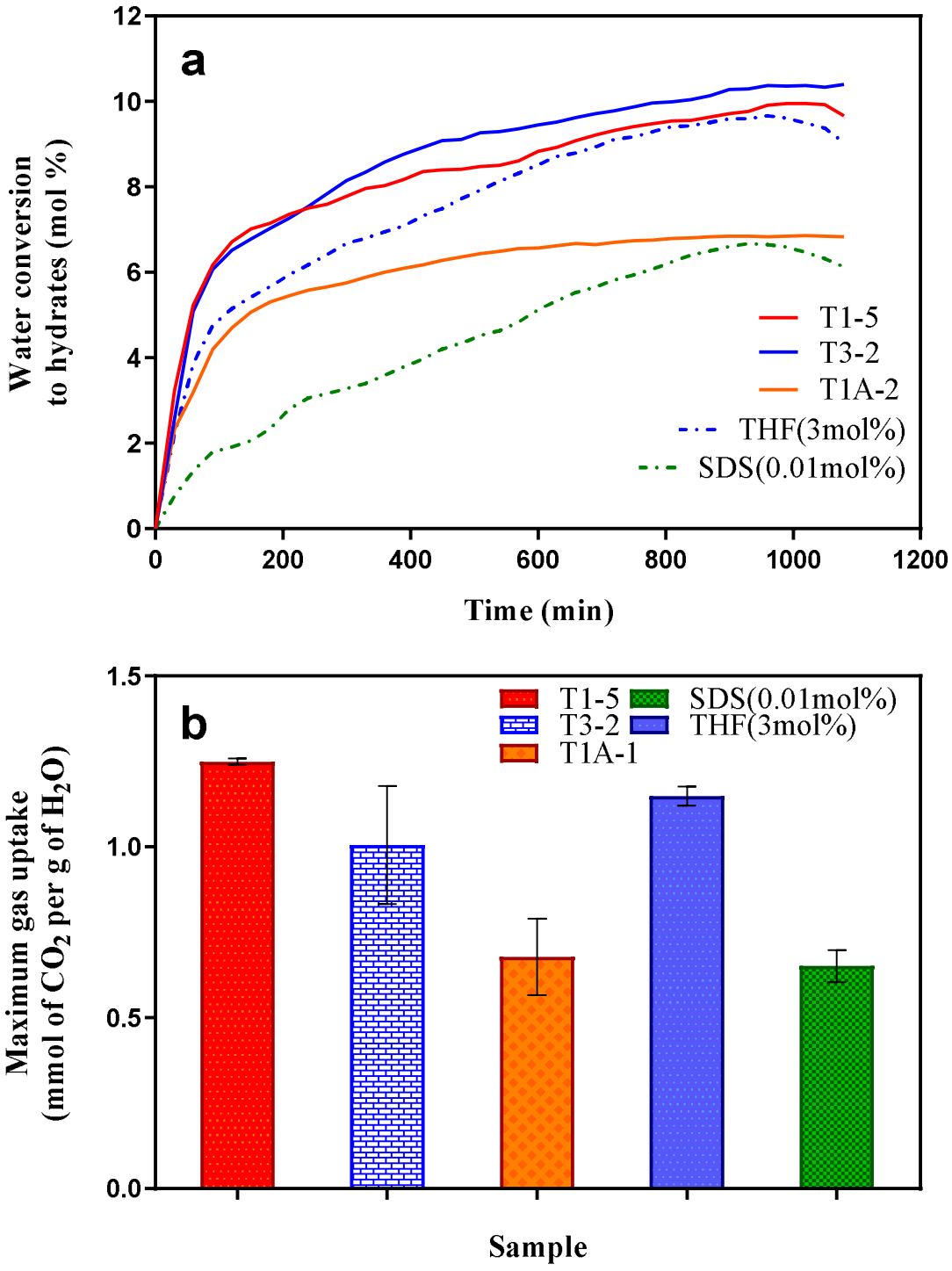

Fig. 7. The comparison of experiments at 288 K and 36 bar in 1200 min; (a) Water conversion to hydrate, (b) Gas uptake for T1-5, T3-2, T1-A and baseline.

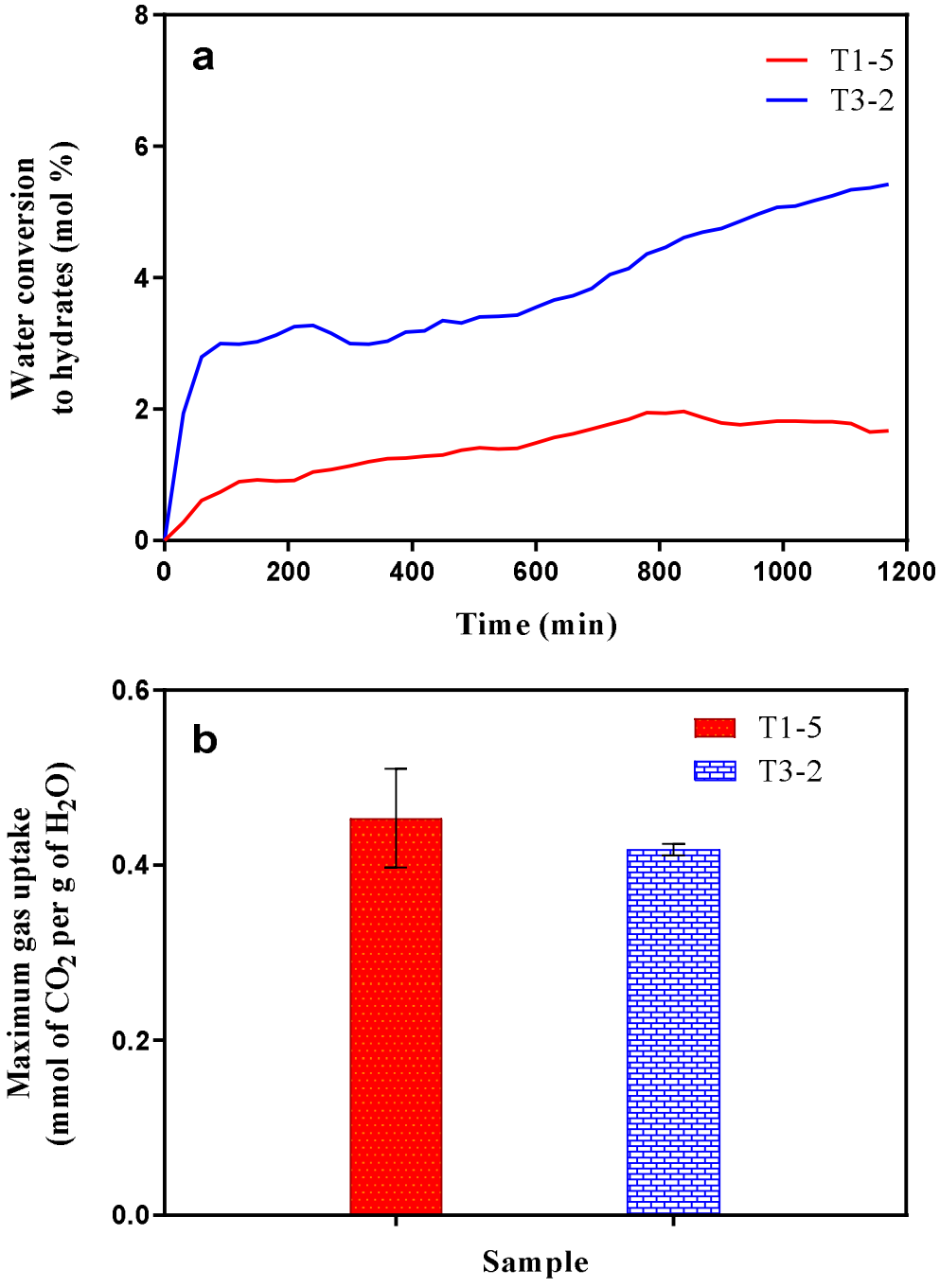

Fig. 8. The comparison of experiments at 293 K and 36 bar in 1200 min; (a) Water conversion to hydrate, (b) Gas uptake for T1-5 and T3-2.

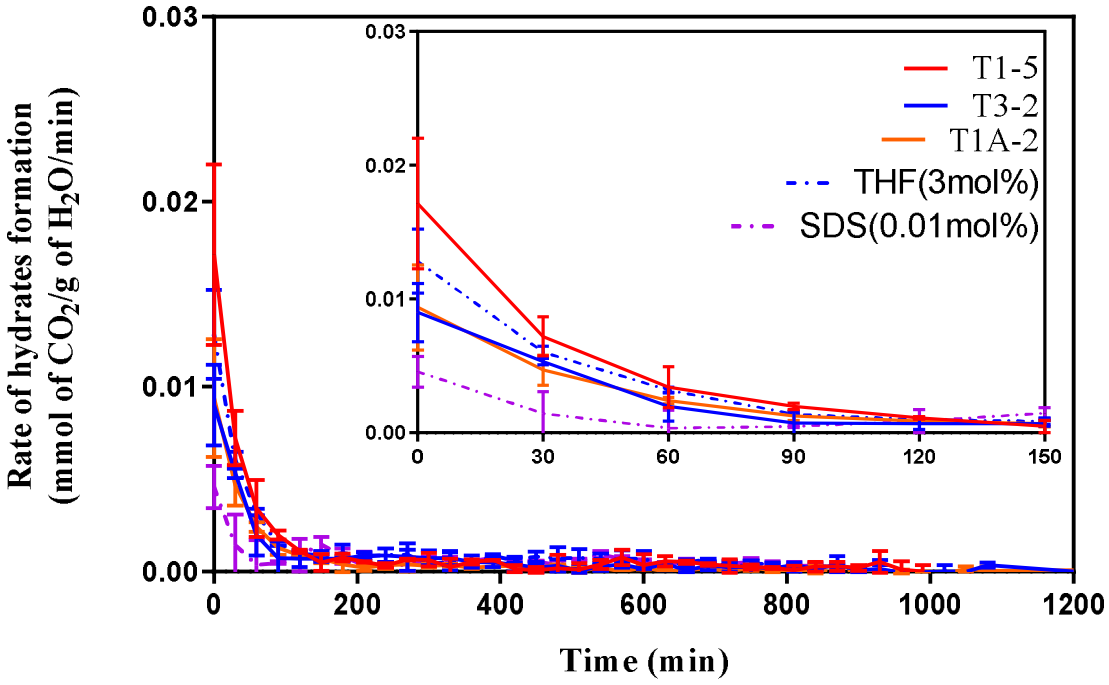

Fig. 9. Rate of hydrate formation at 288 K and 36 bar for 1200 minutes and inset for the first 150 minutes (T1-5, T3-2, T1A-2 and baseline experiments).

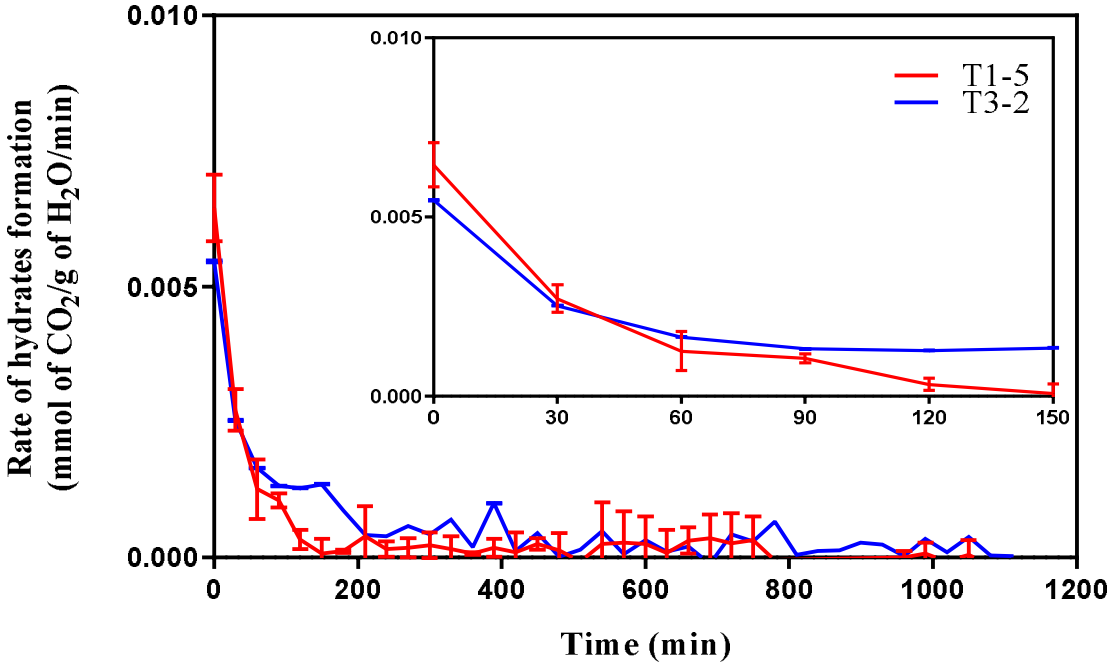

Fig. 10. Rate of hydrate formation at 293 K and 36 bar for 1200 minutes and inset for the first 500 minutes (T1-5 and T3-2).

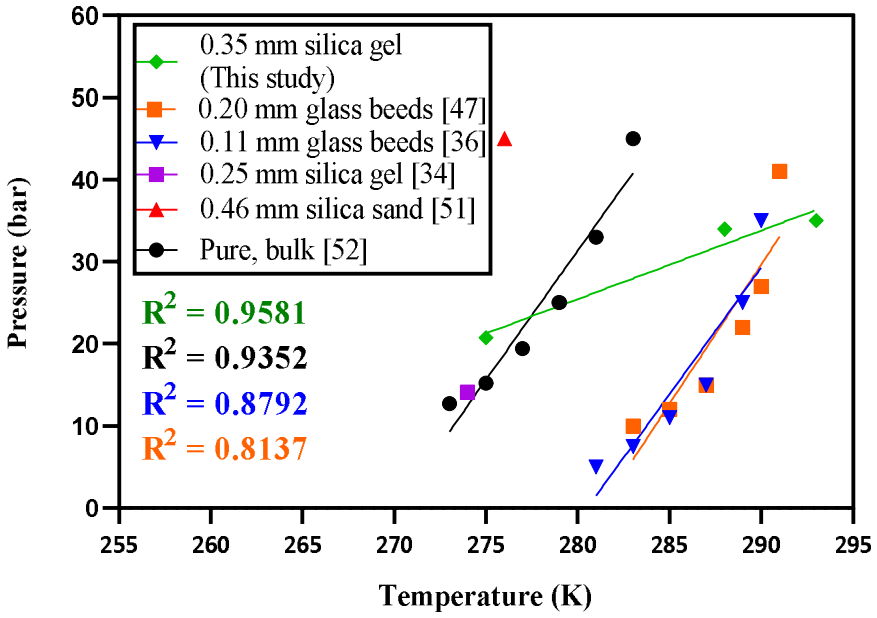

Fig. 11. Comparison of hydrate phase equilibrium of pure CO_2 gas of this study with Yang et al. [52], Yang et al. [39], Kumar et al. [37], Mekala et al. [56] and Carrol work [57].